

## Impurity Transport Study Using Radial Profiles of Fe n=3-2 L $\alpha$ Transition Array Measured by Space-resolved EUV Spectrometer in LHD

LHDにおける空間分布計測用EUV分光器による鉄n=3-2 L $\alpha$ 遷移の径方向分布計測に基づいた不純物輸送研究

Xianli Huang<sup>1</sup>, Shigeru Morita<sup>1,2</sup>, Tetsutarou Oishi<sup>1,2</sup>, Motoshi Goto<sup>1,2</sup>, Hongming Zhang<sup>1</sup> and Izumi Murakami<sup>1,2</sup>

黄賢礼<sup>1</sup>, 森田繁<sup>1,2</sup>, 大石鉄太郎<sup>1,2</sup>, 後藤基志<sup>1,2</sup>, 張洪明<sup>1</sup>, 村上泉<sup>1,2</sup>

<sup>1</sup> Department of Fusion Science, Graduate University for Advanced Studies, Toki 509-5292, Gifu, Japan

<sup>2</sup> National Institute for Fusion Science, Toki 509-5292, Gifu, Japan

<sup>1</sup> 総合研究大学院大学 核融合科学専攻 〒509-5292 岐阜県土岐市下石町322-6

<sup>2</sup> 核融合科学研究所 〒509-5292 岐阜県土岐市下石町322-6

The Fe n=3-2 transition array consisting of Fe<sup>16+</sup> through Fe<sup>23+</sup> ions is utilized for impurity transport study in the Large Helical Device (LHD). The impurity transport can be studied without any assumption on the radial structure of transport coefficients. A one-dimensional transport code is employed to simulate the emissivity profile of iron line emissions. The transport coefficient is then determined by fitting the measured profile with the impurity transport code. Result of the iron transport analysis in high and low electron density discharges is reported. An effect of electron density and temperature gradients on the transport is also discussed.

### 1. Introduction

In LHD the density profile can easily exhibit a peaked, flat or hollow shape, depending on plasma conditions such as  $B_t$ ,  $T_e$ , and  $n_e$ . Therefore, it is of great interest to investigate corresponding impurity transport in the plasma core of LHD [1-2].

For the purpose of impurity transport study, the Fe n=3-2 L $\alpha$  transition array in the narrow wavelength range of 10 – 18 Å is of great advantage because the transition array includes emissions from ions in several charge states of Fe<sup>16+</sup> through Fe<sup>23+</sup>. The iron transport can be analyzed along the minor radius without any assumption on the radial structure of transport coefficients because the Fe L $\alpha$  transition at several ionization stages is emitted over a wide range of the radial plasma location.

### 2. Experimental setup

An extreme-ultraviolet (EUV) spectrometer [3] working in the wavelength range of 10-130Å is used for this study. It measures upper half profile of the elliptical LHD plasma as shown in Fig. 1.

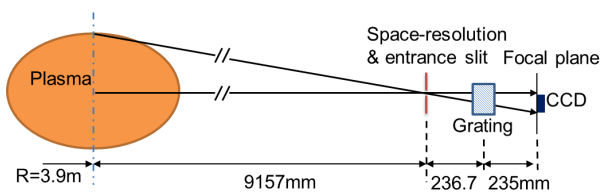


Fig.1. Schematics of the EUV system

### 3. Transport simulation

A one-dimensional impurity transport code is employed to determine the transport coefficient. It is assumed that the impurity transport satisfies the following equation:

$$\Gamma_q = -D_q(r) \partial n_q / \partial r + V_q(r) n_q, \quad (1)$$

where  $\Gamma_q$ ,  $n_q$ ,  $D_q$  and  $V_q$  are the particle flux, the ion density, the diffusion coefficient and the convective velocity of impurity ions in the  $q$ th charge state, respectively.

### 4. Transport analysis

Figure 2 shows waveforms of  $P_{\text{NBI}}$ ,  $n_e$ ,  $T_e$ ,  $P_{\text{rad}}$ ,  $W_p$  and the intensity of the Fe L $\alpha$  array in a discharge with magnetic axis position of  $R_{\text{ax}} = 3.6\text{m}$  and a relatively low density of  $n_e < 5 \times 10^{13} \text{cm}^{-3}$ . The emission profile is measured in the time frame denoted with hatched region in Fig. 2. The intensity of Fe L $\alpha$  emissions starts to increase at  $t = 4.2\text{s}$  after switching off NBI#2 beam. It strongly indicates the iron ion accumulates into the plasma core.

The measured and simulated emissivity profiles are plotted in Figs. 3(a) -(c). The transport code can well reproduce the profile with radial structures of the transport coefficients shown in Fig. 7(d). The diffusion coefficient of  $0.06 \text{m}^2/\text{s}$  seen in the periphery region of  $0.6 \leq \rho \leq 1.0$  is significantly smaller than the value of  $0.2 \text{m}^2/\text{s}$  seen in the

plasma core. The reduction of  $D$  may be related to an increase in the collisionality at the edge region [4]. A weak outward convection,  $V = 0.5$  m/s, is observed near the plasma center of  $0.12 \leq \rho \leq 0.36$ . This may be due to a positive gradient in the density profile. In the outer region of  $0.36 \leq \rho \leq 1.0$ , the convection is inversely changed and becomes inward. A detailed analysis on the radial structure of the convection velocity may require the information on the radial electric field, which sometimes plays an important role in the formation of impurity convection [5].

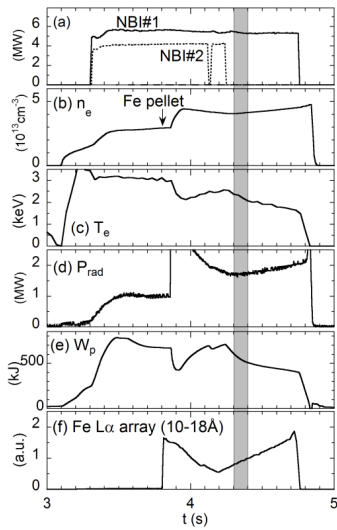


Fig.2. Waveforms of discharge #118639

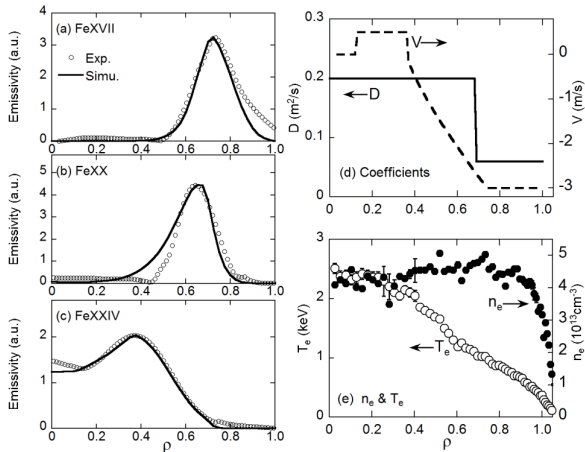


Fig.3. Measured and simulated profiles of (a) FeXVII at  $15.02\text{\AA}$ , (b) FeXX at  $12.80\text{-}12.90\text{\AA}$  and (c) FeXXIV at  $10.62\text{-}10.66\text{\AA}$ , (d) profiles of diffusion coefficient and convective velocity and (e) profiles of  $n_e$  and  $T_e$ .

In comparison with Fig. 3, the transport analysis in high-density discharges is shown in Fig. 4. The  $D$  is constant along the minor radius, while the  $V$

increases the inward convection velocity toward plasma outer region and then keeps constant in the plasma periphery ( $0.75 \leq \rho \leq 1$ ). The structure of  $V$  seems to change against the density profile.

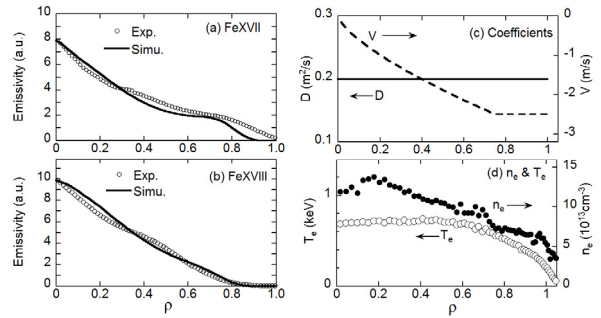


Fig.4. Transport analysis in high-density discharge.

Figure 5 shows the iron transport in plasmas with  $R_{ax} = 3.75\text{m}$  and ECH off-axis heating. A weak inward convection is observed in the plasma core, while the convection disappears in the outer region of  $0.6 \leq \rho \leq 1.0$  where the ECH wave is deposited. It strongly suggests the temperature gradient gives an effect on the impurity transport.

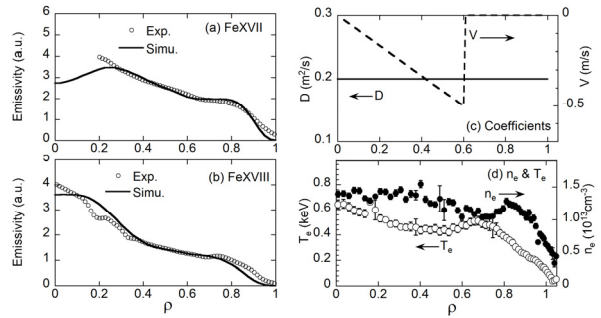


Fig.5. Transport analysis in a plasma heated by off-axis ECH.

## Acknowledgments

This work was partially supported by the LHD project financial support (NIFS14ULPP010) and the JSPS-NRF-NSFC A3 Foresight Program in the field of Plasma Physics (NSFC: No.11261140328, NRF: No. 2012K2A2A6000443).

## References

- [1] S. Morita, *et al.*, Plasma Sci. Technol. **8** (2006)55.
- [2] M. Yoshinuma, *et al.*, Nucl. Fusion **49** (2009) 062002.
- [3] X. L. Huang, S. Morita, T. Oishi, M. Goto, and C. F. Dong, Rev. Sci. Instrum. **85** (2014) 043511.
- [4] S. Murakami, *et al.*, Nucl. Fusion **42** (2002) L19.
- [5] K. Ida, *et al.*, Nucl. Fusion **45** (2005) 391.